Optimization of a Water Window Capillary Discharge Radiation Source

M. Stefanovič, M. Vrbová

Abstract

Computer modeling of a fast electrical discharge in a nitrogen-filled alumina capillary was performed in order to discover discharge system parameters that lead to high radiation intensity in the so-called water window range of wavelengths (2–4 nm). The modeling was performed by means of the two-dimensional RMHD code Z*. The time and spatial distribution of plasma quantities were used for calculating the ion level populations and for estimating the absorption of the 2.88 nm radiation line in the capillary plasma, using the FLYCHK code. Optimum discharge parameters for the capillary discharge water window source are suggested. The heating of the electrodes and the role of capillary channel shielding were analyzed according to the Z* code.

Keywords: water window radiation, capillary discharge, soft X rays, nitrogen plasma.

1 Introduction

2 RMHD computer modeling

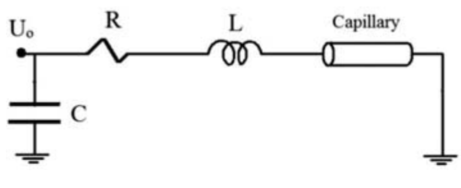

Fig. 1: Electrical scheme of the capillary discharge circuit

2.1 Code input

2.1.1 Electrical scheme of the discharge system

$C = 15$ F, $U_0 = 80$ V, $R = 0.73\ \Omega$, $L = 50$ H

2.1.2 Capillary discharge geometry and filling gas

$\mu/\mu_0 = 8.5$, $A = 102$, $(Z = 7, A = 14)$, $(Z = 26, A = 55.8)$, (0.8, 1.65, 2.5), ~ 0.6

c a . T c a
c c b a
. P a a c-
a b .

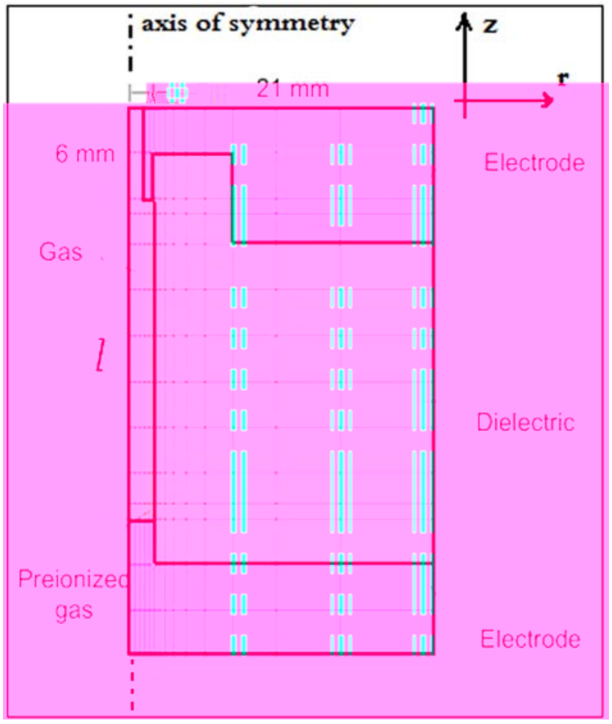

Fig. 2: Capillary grid in 2D cylindrical geometry

T (F 2) c
ac c a a c ca a a
ca c . T a a a
a a- c a a -ca a
b a . T c ca a a -
c b 9 a , c .
N a a c c a
a 2 3 .
A , a a [5] c fi a a
a . T a a
a a ca a a a ∼ 300 K.
A - a a c a " ff c -
a " $Z \sim 10^{-3}$ a c -
a ∼ 0.05 V b c a a
c a a a a . Ca c a
a a a c a a
a 13 667 Pa.

2.2 Results of modeling

2.2.1 Spatial and time distributions of plasma quantities

W a c a ca ac c c ca -
a c a , c c c a a a -
c a , a fi ca a a
c H a a a a
c a c . T a a a

b a a a a -
a , a a ,
c a a . fi a . F 3 -
a b a a c -
a = 85 , a c .
T a z c-
, a c a a a c-
. O a , a c
a 10^{17} c $^{-3}$. T c a
b a b a ca a
(0 c < r < 1) a a a a
T ∼ 50 V (F 4).

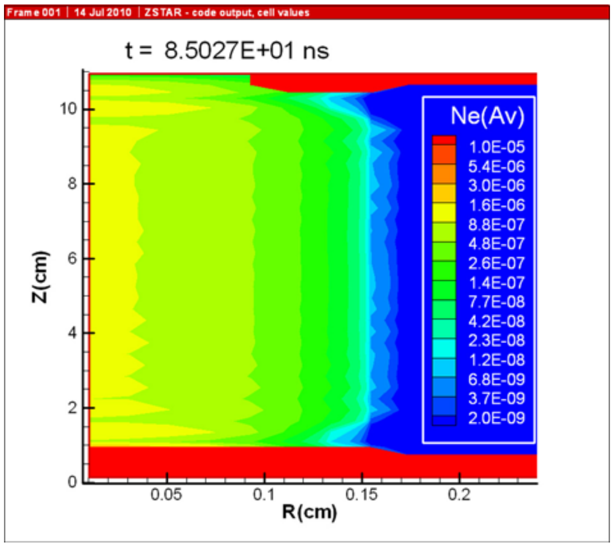

Fig. 3: Radial and longitudinal distribution of electron density Ne at time $t = 85$ ns (the units in the figure are given in Av; density expressed in cm^{-3} may be obtained by multiplying the value by the Avogadro constant $Na = 6.02 \times 10^{23}$)

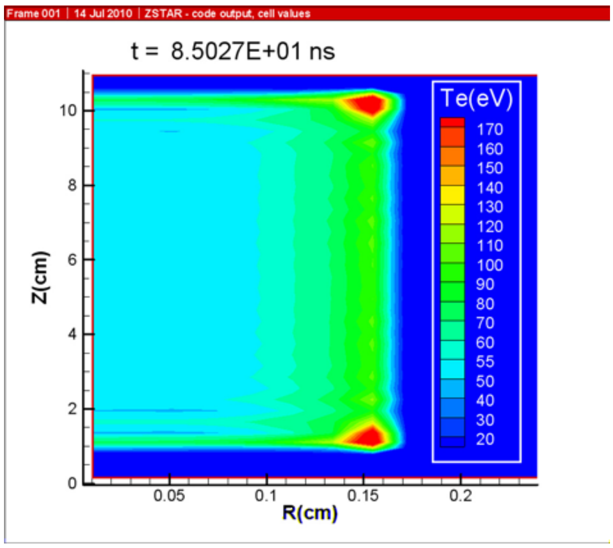

Fig. 4: Radial and longitudinal distribution of electron temperature Te at time $t = 85$ ns

2.2.2 Output radiation estimated by the Z* engine

T c a
a a ca a ,
20 ff c a . A a -
a a a ,
b 13
Z* c , c a a
$2.1 < \lambda < 3.1$. W b
ca a a a fi c a a
$p_m = 80$ Pa. F 5 a -
a a a (c a a)
P_{rad} a ca a . T fi a a a
ac a ~ 15 , a c a ,
c , a a a $t \sim 85$. T c
a a c . T a a c-
a 13 (P_{euv}) a a a
c . I a a 3 a
a a a a a P_{rad}. T a a
a c a a c a .

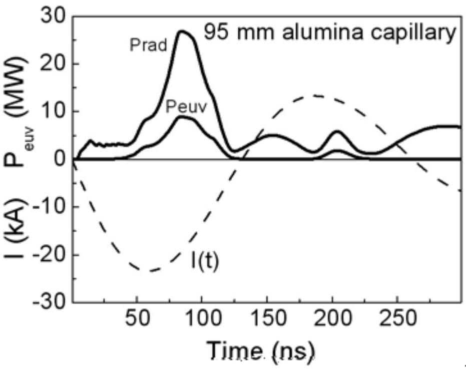

Fig. 5: Time dependences of evaluated electric current (dashed line), total radiation P_{rad} and radiation P_{euv} in the selected group 13

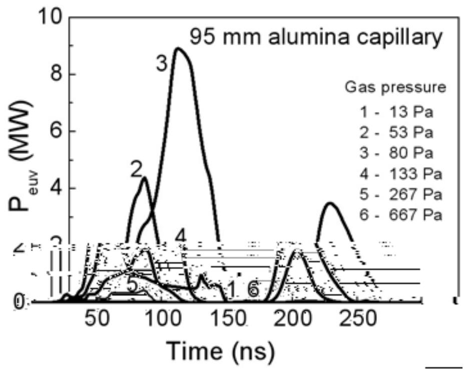

Fig. 6: Time dependencies of radiation power P_{euv} in group 13 for various initial gas pressures

A , a a a a -
a 13 667 P c
a 1.65 ca a a , fi -
fi a . T a a a

c a a a ,
a F 6. T a a
a ac a a 80 Pa a
85 . T fi
a ca a a $r = 1.65$. A ca -
a $l = 95$ c , b a
a b a
a ca a 40 180 .
T a c fi a
a a ca a a
(0.8 a 2.5). T a F 7.
T F 7
c ca a a . T
a c a c
a ca a .
I c a
a a ca a a ,
ca a ac ca -
a a 0.8 , fi a 400 Pa
(F 8).

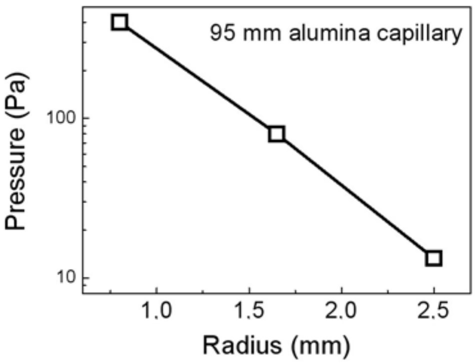

Fig. 7: Dependence of optimal pressure on the radius of the capillary

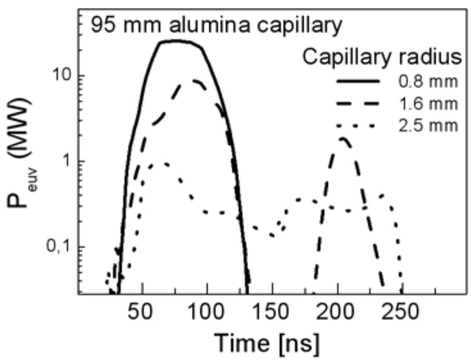

Fig. 8: Pressure optimized time dependences of radiation power P_{euv} in group 13 for different capillary radii

3 Spectrum according to FLYCHK

T - a FLYCHK c [6] a
a c a a a-
ca a . W c

a a fi a a ca a c ($r = 0$ c , $z = l/2$, r a z a a a a) a c a , c , a l ca a). S a c a a a a c c a ca a a 0.3 a , b ca a a a (F 3, 4).

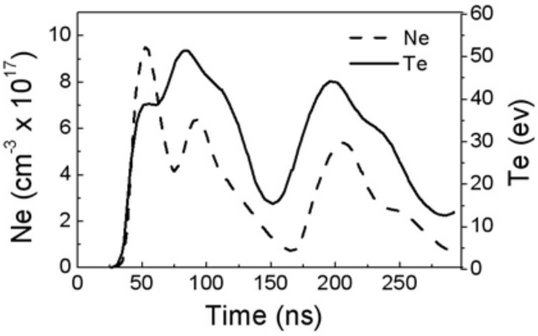

Fig. 9: Time evolutions of electron density and temperature calculated by Z*, for gas pressure 80 Pa

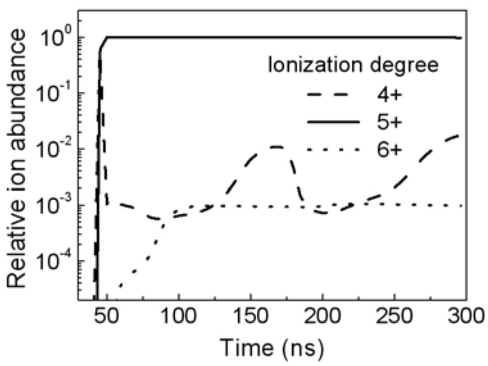

Fig. 10: Time dependences of relative nitrogen ion abundances for initial gas pressure 80 Pa (logarithmic scale)

T c N a c a T a Z* c ca c a (F 9), a c a a fi FLYCHK c . N LTE a a , a a c a c , b ca c McW c [7] LTE a a . O ca c a a 5 c . T a ab a c a 80 Pa a F 10 (4^+, 5^+ a 6^+ ac a , ac a ab a c). I a H N^{5+} a a c a $t \sim 50$.

I a a c a a $t = 85$ $\lambda = 2.1.$ 3.1 a F 11. W a c a a a $\lambda = 2.878\,5$, c a

a 1 2 1 2 , a . T ca ((Io/I)) a 5 a a c ff a c F 12. W a ab 2.88 c a a a, . . a a c c a c c a a a a a . T c c c fi b a E a ca c a ab c ffic [8].

$$k = N_l \frac{g_u}{g_l} \cdot \frac{\lambda^3}{8\pi c \left(\frac{\Delta\lambda}{\lambda}\right)} A_{ul}$$

W ab c ffic , g_u a g_l a a ca a a c , c , N_l b , λ a a , $\Delta\lambda$ D b a , a c . P $\Delta\lambda/\lambda = 1.45 \times 10^{-4}$ [8], ca c a a ab c ffic $k = 110$ c $^{-1}$, c a b 5 c a a FLYCHK.

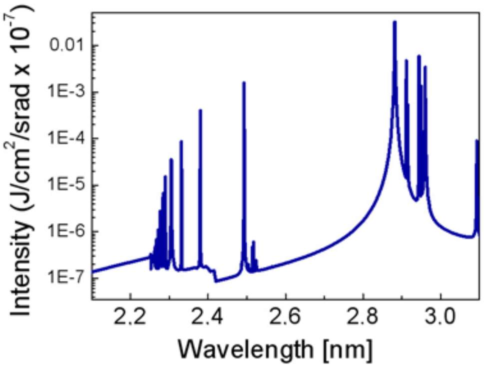

Fig. 11: Spectra for filling gas pressure 80 Pa at the time of maximum output radiation $t = 85$ ns

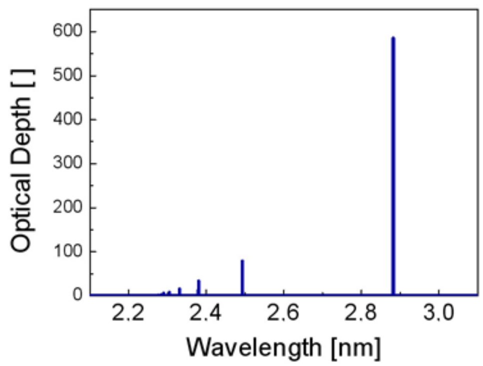

Fig. 12: Optical depth of the 5 cm plasma channel for gas pressure 80 Pa at the time of maximum output radiation $t = 85$ ns

4 Electrode heating

A Z* a a c dT_{el}, b a . W a a c

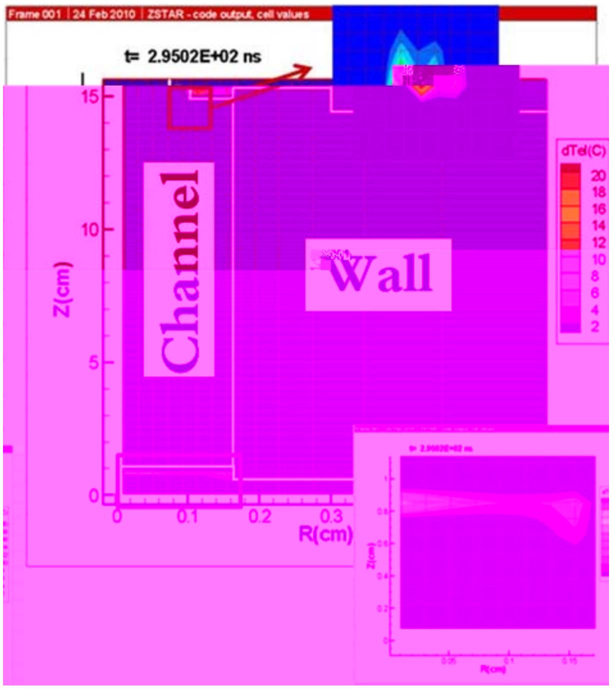

Fig. 13: Temperature increase of the electrodes for the discharge system with the tip drawn into the channel, after 300 ns from the beginning of the discharge; most heated parts are magnified

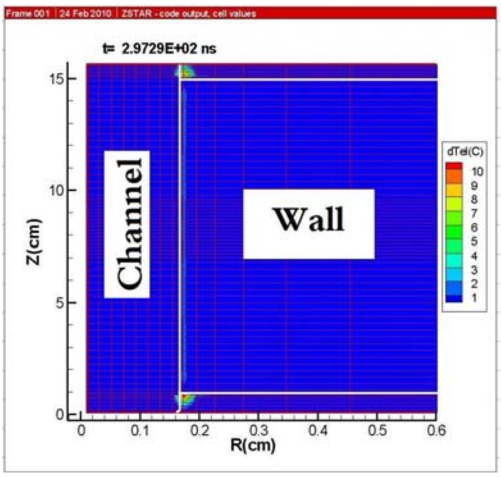

Fig. 14: Temperature increase of the electrodes for the discharge system with electrodes in the line with the capillary wall 300 ns after the beginning of the discharge

5 The role of capillary shielding

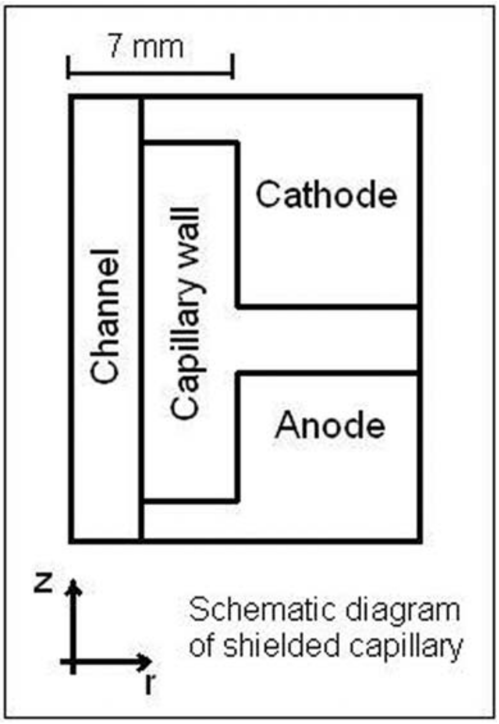

Fig. 15: Schematic diagram of a shielded capillary, represented in a cylindrically symmetrical geometry

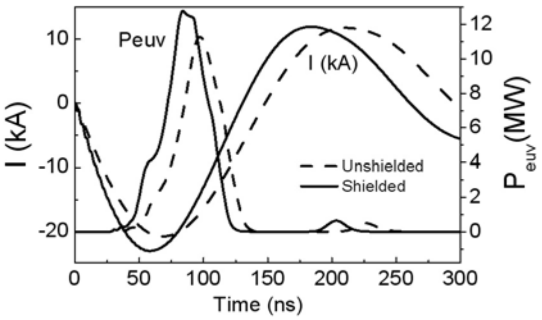

Fig. 16: Time dependences of the output radiation power in group 13 and the current for a shielded capillary (full line) and for an unshielded capillary (dashed line)

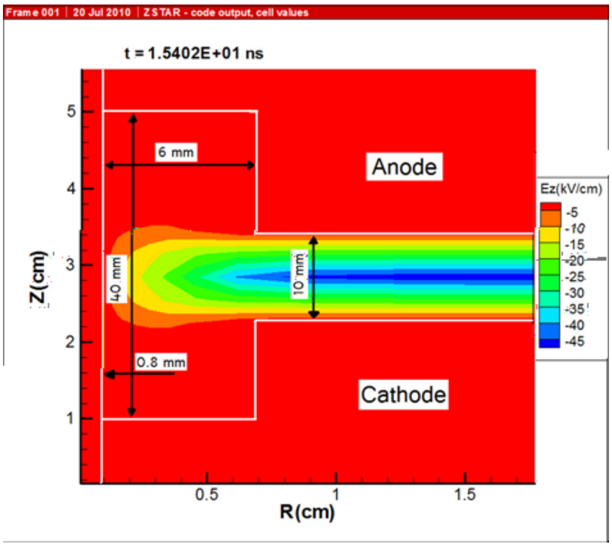

Fig. 17: Distribution of the z-component of the electric field in the discharge for the proposed geometry of the discharge (the axes are not proportional)

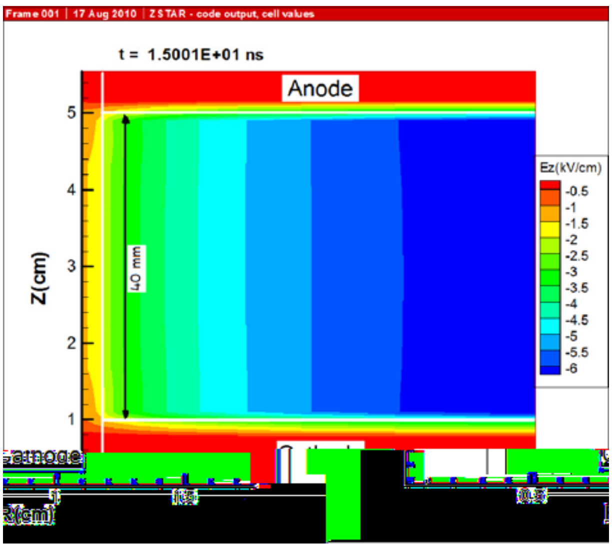

Fig. 18: Distribution of the z-component of the electric field in the discharge for the proposed geometry of the discharge (the axes are not proportional)

a 15 (c fi ac a acc Z*-c) a a ca a 4 c (a a c c c fi b c a z c). T c ca fi ac a a a 45 V/c a ca a (F 17), a 6 V/c a - ca a (F 18). S c c ca b a - a cc a c c fi 30 V/c , c c a c b a (b c c b a a a a (. . a a)) a c a a ca a .

6 Suggested parameters of the new source

W a a a ca a c a a a a c ba c c b ab . T c ca a a c a a b a : ca-ac $C = 15$, a $U_0 = 80$ V, - a $R = 0.73\ \Omega$, a a c a c $L = 50$ H.

Ca a a 0.8 ab a c a 400 Pa. T ca a c a b 4 c ab a a a a a c . D c c fi a a ca a , a a ca a b a c . T - c a F 18. T c c a a a- Z* 13 a a - a F 19. T XUV cc a a c a , c a 50 . T c a a b - a a a F 20 a 21. T c a c , c a a a c T c a a b a ca a - a a a 70 V, ab c a N^{5+} .

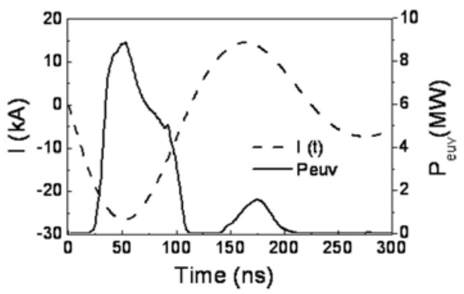

Fig. 19: Time dependences of the output radiation power in group 13 and the current for the proposed geometry

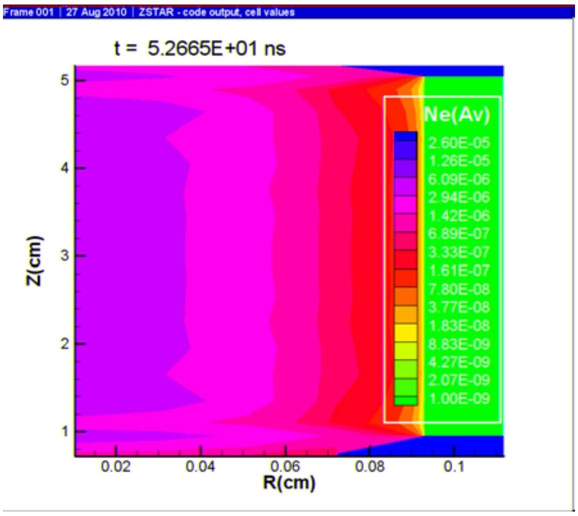

Fig. 20: Radial and longitudinal distribution of electron density Ne at the time of maximum current (the units in the figure are given in Av; the density expressed in cm^{-3} can be obtained by multiplying the value by the Avogadro constant $Na = 6.02 \times 10^{23}$)

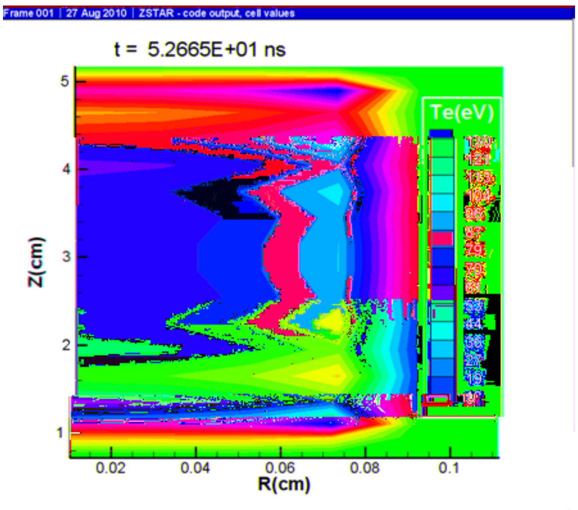

Fig. 21: Radial and longitudinal distribution of electron temperature T_e at the time of a current maximum

7 Conclusions

T RHMD Z* c a a ca a c c a a c a c " a " a a c . T a a- 13 (2.1 3.1 a - a ff a a , ff ca - a a a ff ca a . T - a a (0.8), fi a a 400 Pa ca a 40 U FLYCHK c a a - c , a c c a ab a c a a . A 50 , N^{5+} c . FLYCHK a ab

2.88 a a a a. E c a a a ff c a c f a . T ca a a a b Z*.

Acknowledgement

T a a a S Za a a c Z* c a c c a . T a c a b MEYS R a c P c C42 a b MEYS R a c P c INGO LA 08024.

References

[1] F , T. W.: I C U S X a . I : *From Cells to Proteins: Imaging Nature across Dimensions*, A a : S N a , 2005, . 167 185.

[2] Za a , S. V., N , V. G., C , P.: Z*- c DPP a LPP c . I : *EUV Source for Lithography.* (E . V. Ba). B a , Wa : SPIE PRESS, 2005, . 223 275.

[3] Za a , S. V., N , G. V., M , M., C , P P a a D a c H Ca T D c a I fl c Fa E c- I a P a a EUV E - . *Plasma Sources Sci. Technol.* **17** (2), 2008, . 13.

[4] N a, M.: *Návrh a realizace zařízení pro studium kapilárního výboje v argonu: Diplomová práce.* P a a : VUT Fa a a á a á á, 2008.

[5] V ba, a .: *Capillary pinching discharge as water window radiation source.* 29 ICPIG, Ca c , M c , 2009.

[6] L R. W., La , J. T.: A - a a c c K- - , *JQSRT* **56**, 1996, . 535 556.

[7] McW , R. W. P I : *Plasma Diagnostic Techniques?* (E . R. H. H , S. L. L a), Aca c P , N Y , 1965, . 201 264.

[8] E , C. R.: *X ray lasers.* L : Aca c P , 1990.

I . M S a
P . M a a V b á, CSc.
E- a : stefanovic@fbmi.cvut.cz
D a N a Sc c
Fac B ca E
C c T c ca U P
. S 3105, K a 2, C c R b c